Drivers of convection initiation in the Tropical Andes

Diego Urdiales-Flores[1], Francina Dominguez[2], Divyansh Chug[3], Grégoire Mariéthoz[1,4], Charles Jones[5], Leila M.V. Carvalho[5], and Nadav Peleg[1,4]

[1]Institute of Earth Surface Dynamics, University of Lausanne, Lausanne, Switzerland
[2]Department of Climate, Meteorology, and Atmospheric Sciences, University of Illinois Urbana-Champaign, Urbana, IL, USA
[3]Aon Impact Forecasting
[4]Expertise Center for Climate Extremes, University of Lausanne, Lausanne, Switzerland
[5]Department of Geography, University of California, Santa Barbara, CA, USA

Correspondence: Diego Urdiales-Flores (diego.urdialesflores@unil.ch)

Supplementary Table 1. Distribution of CI event durations [hours] by eco-region.

Eco-region	Percentile 25th	Percentile 50th	Percentile 75th
NAMZ	0.5	1	3.5
ANDES-L	1.5	3	4.6
ANDES-H	0.5	1	3
COAST	2	6	8

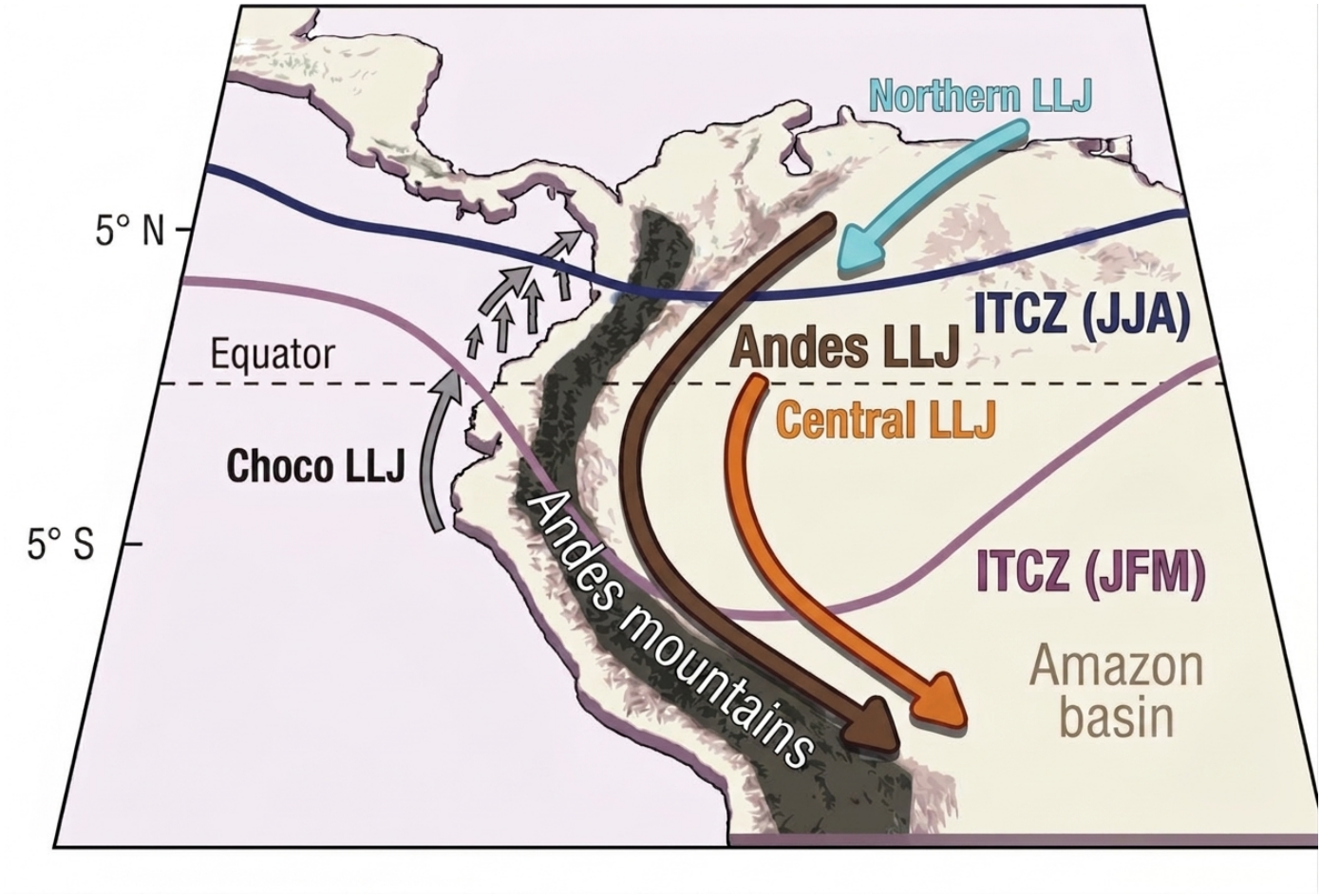


Figure S1. Schematic representation of low-level jets (LLJs) pathways across northern and central South America (adapted from Espinoza et al., 2020). The diagram depicts the spatial distribution of low-level moisture transport channels, showing the Pacific cross-equatorial inflow (Choco LLJ) west of the Andes alongside the Amazonian and eastern-slope trajectories (Andes and Central LLJs) East of the Andes.

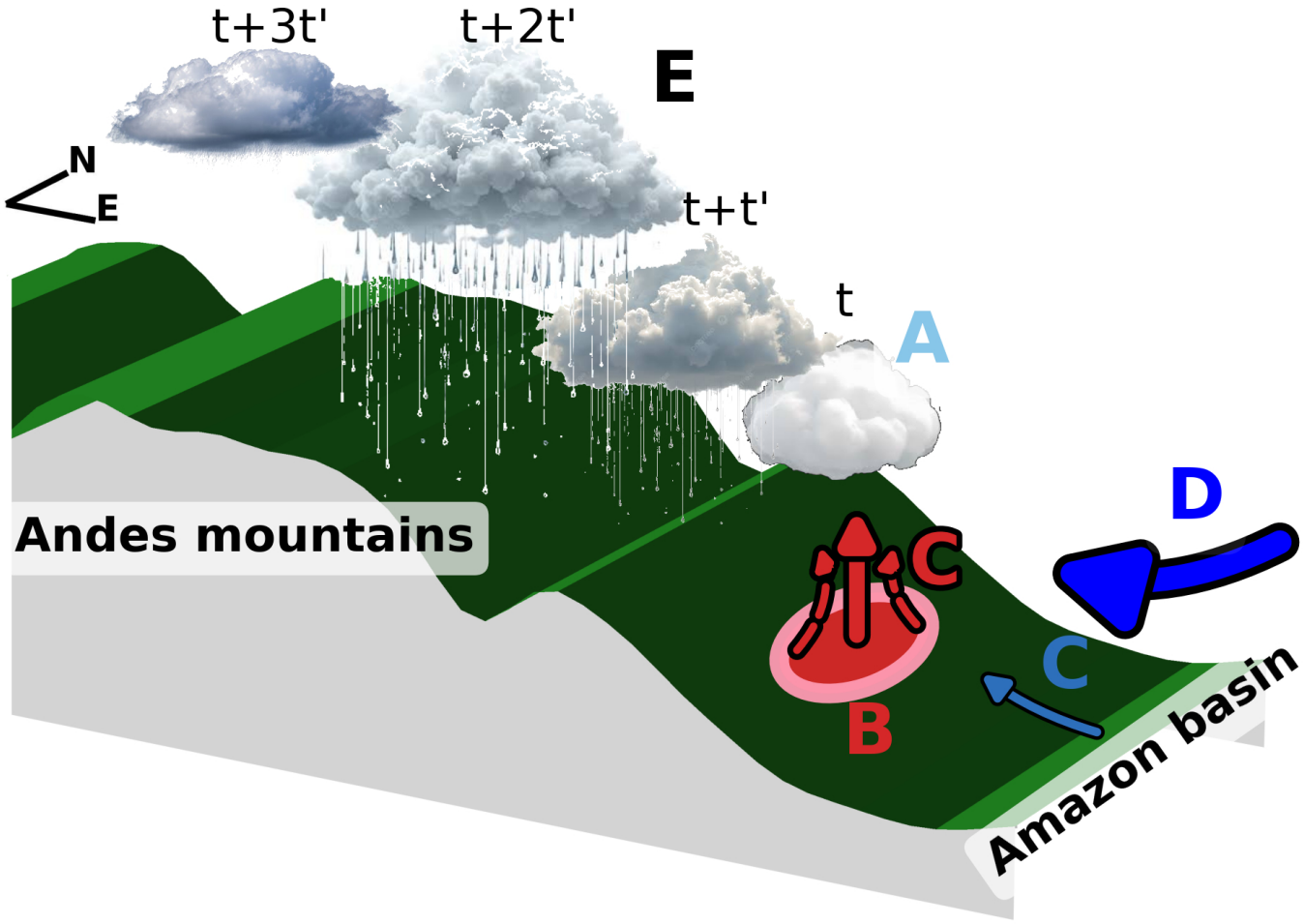


Figure S2. Schematic illustration of convective rainfall development and the methods employed to characterize local and large–scale atmospheric drivers of convection initiation events in the Tropical Andes and their precipitation properties.

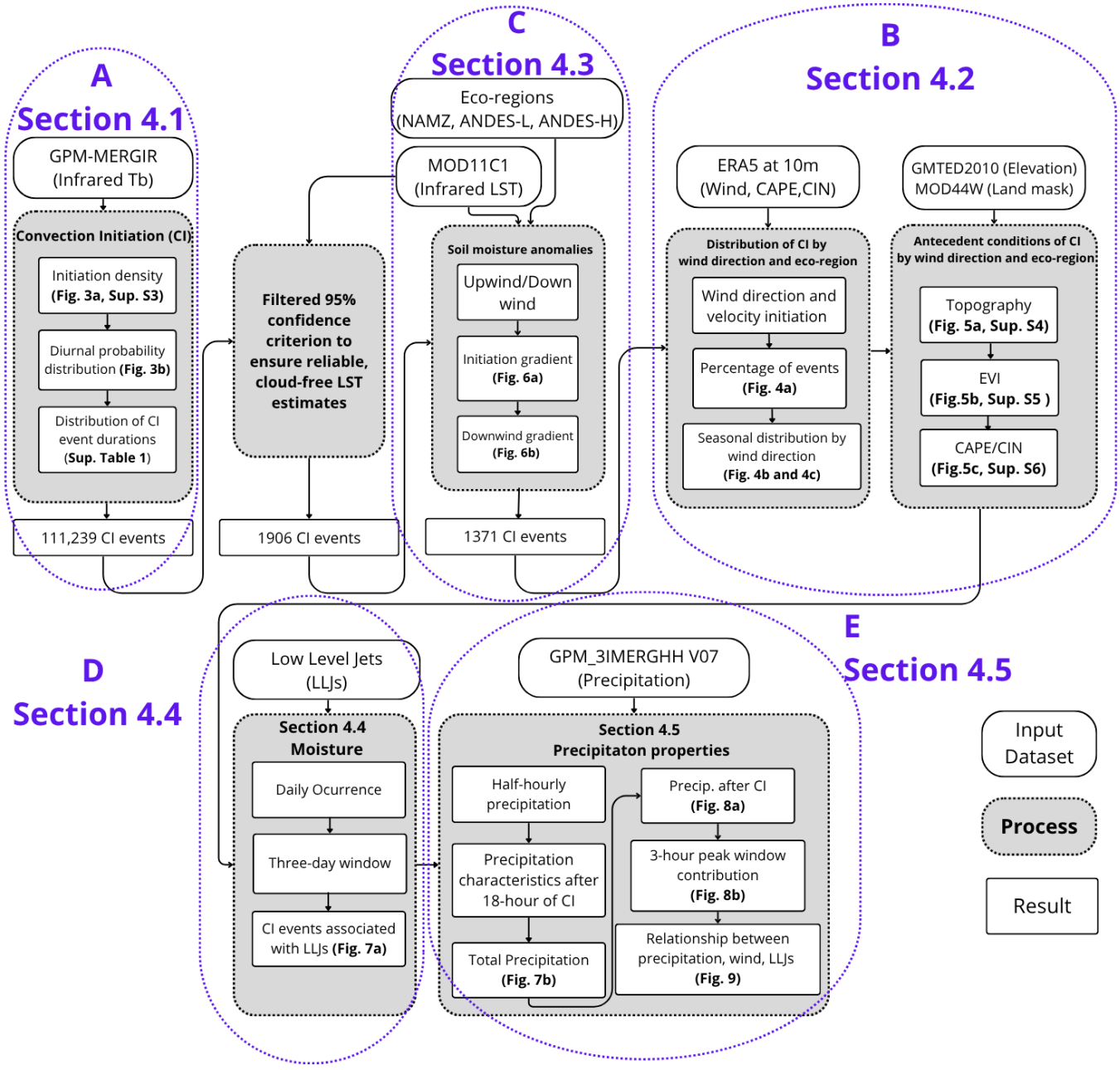


Figure S3. Master schematic illustration of convective rainfall development and the methods employed to characterize local and large–scale atmospheric drivers of convection initiation events in the Tropical Andes and their precipitation properties that describes all these steps, the inputs and outputs. The corresponding sections are described in Fig. 2 and the Methodology.

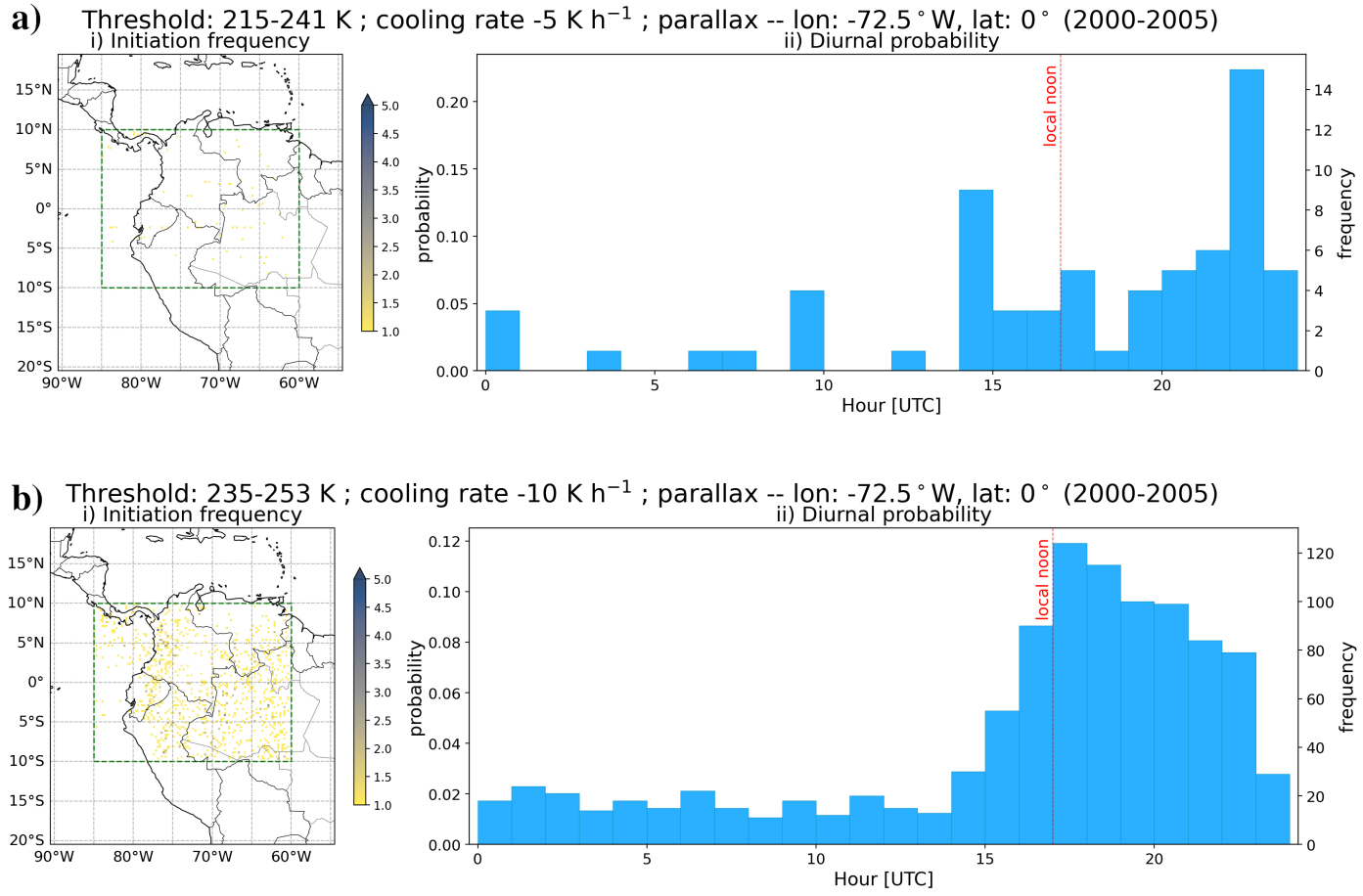


Figure S4. Sensitivity analysis for tracking nascent-stage convective features during 2000-2005. (a) Threshold analysis using a temperature range of 215–241 K and a cooling rate of $-5\,\mathrm{K\,h^{-1}}$. (b) Same as (a), but using a temperature range of 235–253 K and a cooling rate of $-10\,\mathrm{K\,h^{-1}}$.

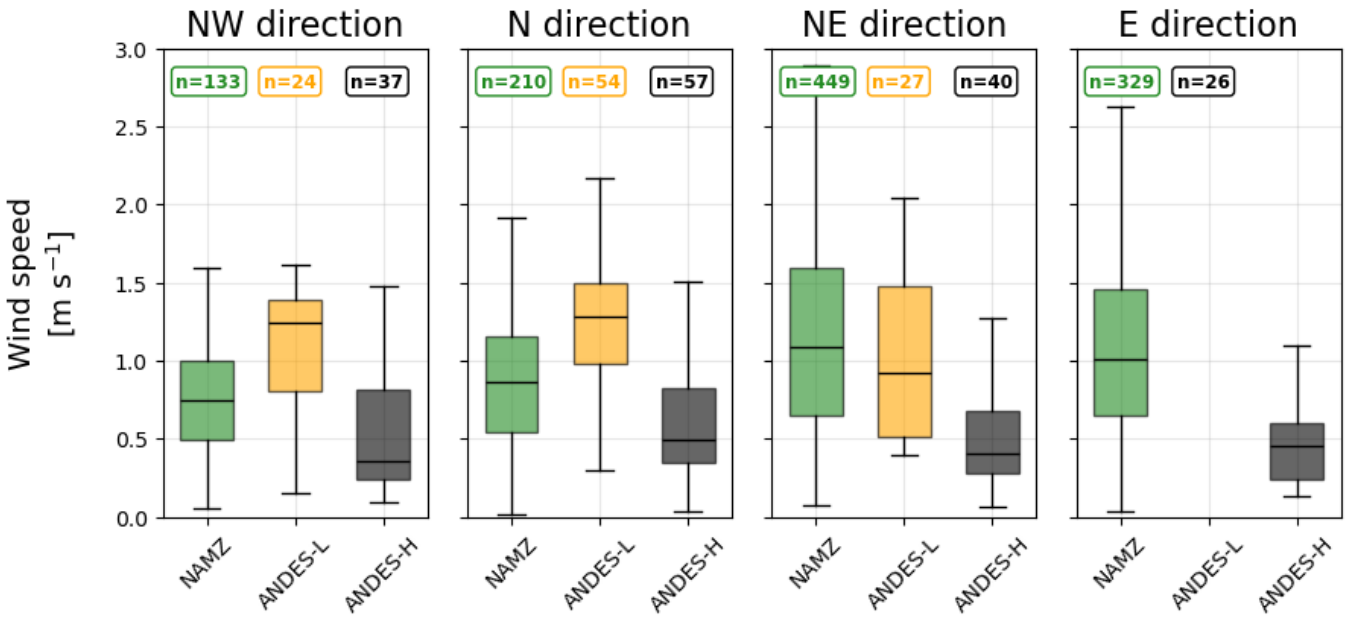


Figure S5. Boxplots of wind speed [m s^{-1}] for the three eco-regions considering wind direction.

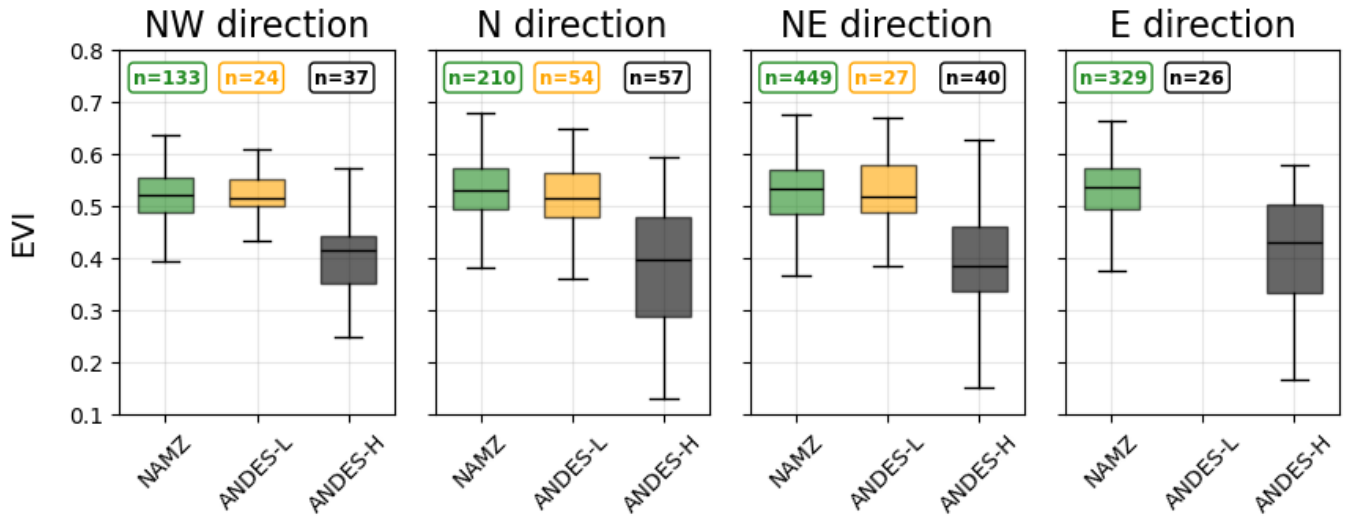


Figure S6. Boxplots of enhanced vegetation index (EVI) for the three eco-regions considering wind direction.

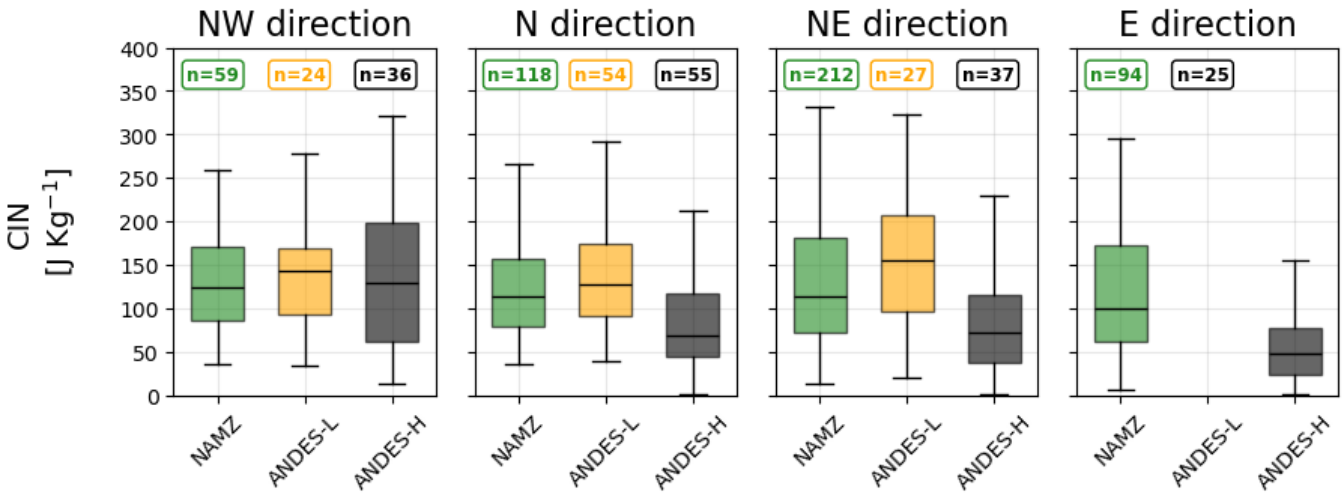


Figure S7. Boxplots of convection inhibition (CIN,[J Kg^{-1}]) for the three eco-regions considering wind direction.

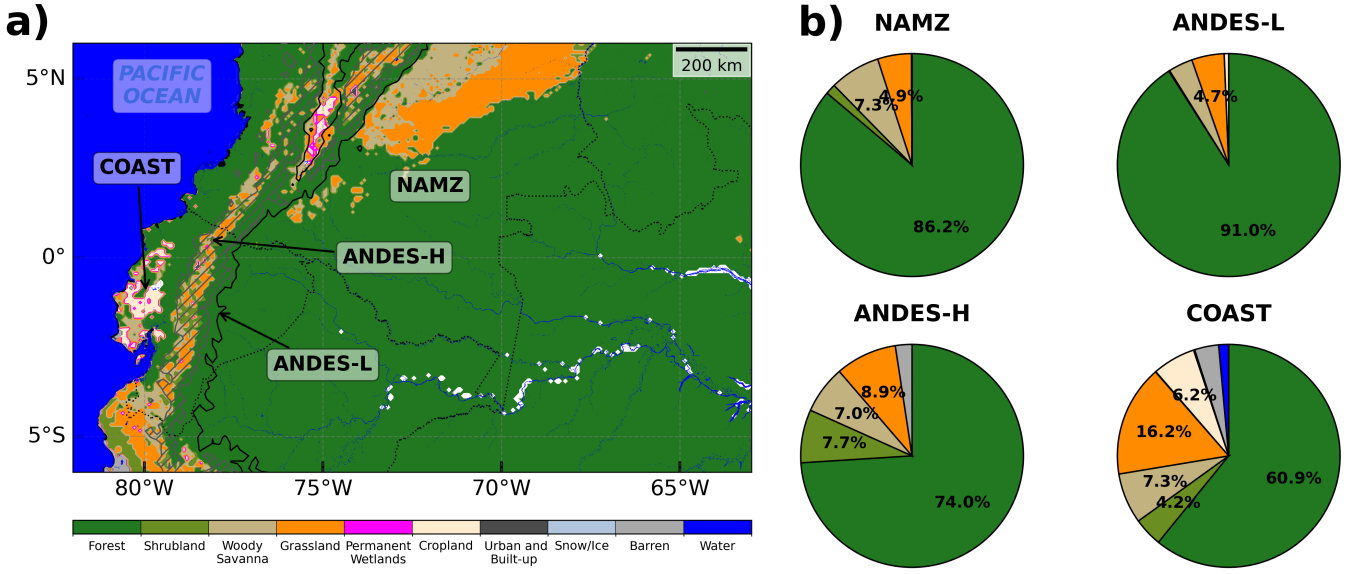


Figure S8. Land-use and Land-cover (LULC) distribution across the study regions based on the 2020 MODIS (MCD12C1 Version 6; https://doi.org/10.5067/MODIS/MCD12C1.006): (a) spatial domain showing target eco-regions (COAST, ANDES-H, ANDES-L, and NAMZ) overlaid on LULC types, and (b) relative proportions [%] of categories within eco-region.

References

Espinoza, J. C., Garreaud, R., Poveda, G., Arias, P. A., Molina-Carpio, J., Masiokas, M., Viale, M., and Scaff, L.: Hydroclimate of the Andes part I: main climatic features, Frontiers in Earth Science, 8, 64, https://doi.org/10.3389/feart.2020.00064, 2020.